Acta Crystallographica Section D
Biological Crystallography
ISSN 0907-4449

Structural asymmetry and intersubunit communication in muscle creatine kinase

Jeffrey F. Ohren,[a]‡ Melisa L. Kundracik,[b] Charles L. Borders Jr,[b] Paul Edmiston[b] and Ronald E. Viola[a]*

[a]Department of Chemistry, The University of Toledo, Toledo, Ohio 43606, USA, and [b]Department of Chemistry, The College of Wooster, Wooster, Ohio 44691, USA

‡ Current address: Pfizer Global Research and Development, 2800 Plymouth Road, Ann Arbor, MI 48105, USA.

Correspondence e-mail: ron.viola@utoledo.edu

Received 27 September 2006
Accepted 22 December 2006

PDB Reference: muscle creatine kinase, 1u6r, r1u6rsf.

The structure of a transition-state analog complex of a highly soluble mutant (R134K) of rabbit muscle creatine kinase (rmCK) has been determined to 1.65 Å resolution in order to elucidate the structural changes that are required to support and regulate catalysis. Significant structural asymmetry is seen within the functional homodimer of rmCK, with one monomer found in a closed conformation with the active site occupied by the transition-state analog components creatine, MgADP and nitrate. The other monomer has the two loops that control access to the active site in an open conformation and only MgADP is bound. The N-terminal region of each monomer makes a substantial contribution to the dimer interface; however, the conformation of this region is dramatically different in each subunit. Based on this structural evidence, two mutational modifications of rmCK were conducted in order to better understand the role of the amino-terminus in controlling creatine kinase activity. The deletion of the first 15 residues of rmCK and a single point mutant (P20G) both disrupt subunit cohesion, causing the dissociation of the functional homodimer into monomers with reduced catalytic activity. This study provides support for a structural role for the amino-terminus in subunit association and a mechanistic role in active-site communication and catalytic regulation.

1. Introduction

Creatine kinase (CK; EC 2.7.3.2) is a member of the guanidino kinase superfamily and catalyzes the reversible transfer of the γ-phosphate from MgATP to creatine to yield MgADP, a proton and phosphocreatine (PCr; Wallimann *et al.*, 1992; Wyss & Kaddurah-Daouk, 2000). This CK/PCr system performs a critical regulatory role in maintaining the intracellular concentrations of ATP, inorganic phosphate (P_i) and protons and is a key component of intracellular energy transport (Ponticos *et al.*, 2004). The regulatory function of CK is particularly important in cells that have large and variable energy demands, such as in the brain, heart and muscle. This important regulatory network has come under additional scrutiny from a number of recent studies suggesting that improper regulation of the CK/PCr system is associated with a variety of disease states, including cardiovascular, neurological, muscle and renal diseases as well as cancer (Schlattner *et al.*, 2006; Wyss & Kaddurah-Daouk, 2000).

The three cytosolic isoenzymes of CK, muscle (MM-CK), brain (BB-CK) and a mixed form (MB-CK), are found as extremely stable dimers (Eder *et al.*, 1999; Wallimann *et al.*, 1992; Wyss & Kaddurah-Daouk, 2000). Mitochondrial CK (MiCK) also forms dimers, which can readily associate to an octameric form depending on the pH and the concentration of MiCK (Kaldis *et al.*, 1994; McLeish & Kenyon, 2005; Wall-

imann *et al.*, 1992). The significant sequence and structural homology within the guanidino kinase family suggests that an ancestral gene may have produced CK, arginine kinase (AK) and the other phosphagen kinase family members (McLeish & Kenyon, 2005). However, in contrast to the CK family, the closely related AKs function almost exclusively as monomers (Fritz-Wolf *et al.*, 1996; Zhou *et al.*, 1998). Despite the higher order association of CK compared with AK, kinetic analysis has not provided evidence to support subunit cooperativity between the active sites of the CK homodimer (Morrison & James, 1965; Suzuki & Furukohri, 1994), although negative cooperativity has been reported for the modification of the active Cys282 with 5′,5′′-dithiobis-2-nitrobenzoic acid (DTNB; Price & Hunter, 1976).

A role in subunit association was suggested for the amino-terminus of MiCK based on mutagenesis experiments, which showed that removal of the five N-terminal residues led to decreased stability of the octameric form (Kaldis *et al.*, 1994). A high-resolution structure of MM-CK confirmed a role for the amino-terminus in subunit contacts (Eder *et al.*, 1999). However, in contrast to these earlier studies, the removal of six residues from the amino-terminus of MM-CK was shown to actually improve subunit association and led to increased stability of the homodimer (Guo *et al.*, 2003). Recently, monomeric MM-CK was generated by mutagenesis of several key residues in the dimer interface (Cox *et al.*, 2003). Monomeric CK has a reduced affinity for its substrates but still retained catalytic activity, demonstrating that dimer association is important but not required for catalysis. Thus, an essential role for the amino-terminus in CK activity and subunit association is still unresolved, providing a rationale for our structural and mutational studies.

The structures of CK and other related phosphagen kinases reveal that the enzyme can exist in one of two primary conformations: an open form with the active site exposed to solvent and a closed form where the active site is shielded. The open form of CK has been observed in a high-resolution structure of the octameric chicken mitochondrial CK (Fritz-Wolf *et al.*, 1996), a moderate-resolution structure of apo rabbit muscle CK (Rao *et al.*, 1998) and a low-resolution structure of apo human muscle CK (Shen *et al.*, 2001). The transition-state analog (TSA) complex structure of *Torpedo californica* CK (*tc*CK–TSA), determined to 2.1 Å resolution, revealed subunit asymmetry as both the open and closed conformations of CK were observed in the homodimeric structure (Lahiri *et al.*, 2002). Additionally, high-resolution structures of the related horseshoe crab *Limulus polyphenus* arginine kinase (*lp*AK) have also been reported in both the open apo and closed TSA-complex conformations (Yousef *et al.*, 2002, 2003; Zhou *et al.*, 1998).

Here, we describe the structure of a TSA complex of a mammalian muscle-type CK, that from rabbit (rmCK), determined to 1.65 Å resolution. This higher resolution structure allows a more detailed examination of the CK subunit asymmetry first observed in the *tc*CK complex structure (Lahiri *et al.*, 2002). When combined with mutagenesis studies of the amino-terminus of rmCK, this study provides new insights into the role of the amino-terminal domain in CK subunit communication and catalytic regulation.

Table 1
Crystallographic data-collection and refinement statistics.

Values in parentheses are for the highest resolution shell (1.69–1.65 Å).

Space group	$P2_12_12_1$
Unit-cell parameters (Å)	
a	48.7
b	92.6
c	165.6
Data collection	
Wavelength (Å)	1.000
No. of reflections	326353
No. of unique reflections	85140
Average multiplicity	3.8
Completeness (%)	97.9 (84.8)
$\langle I/\sigma(I)\rangle$	18 (2)
$R_{\rm merge}$ (%)†	6.2 (40.5)
Resolution (Å)	40–1.65
Refinement	
Refinement program	*REFMAC*5
Resolution range (Å)	40–1.65
$R_{\rm work}/R_{\rm free}$ (%)‡	16.7/20.0
Protein/waters/ligands	760 residues/1155 waters/ 2 MgADP/1 creatine/1 nitrate
Deviations from ideal geometry	
Bond lengths (Å)	0.010
Bond angles (°)	1.29
Coordinate errors§ (Å)	0.06

† $R_{\rm merge} = \sum|I - \langle I\rangle|/\sum I$, where I is the intensity of an individual measurement and $\langle I\rangle$ is the mean intensity of this reflection. ‡ $R_{\rm work} = \sum|F_{\rm o} - F_{\rm c}|/\sum|F_{\rm o}|$, where $|F_{\rm o}|$ and $|F_{\rm c}|$ are the observed and calculated structure-factor amplitudes, respectively. $R_{\rm free}$ is the cross-validation R value calculated for 5% of the reflections omitted from the refinement. § Estimated overall coordinate errors based on maximum-likelihood refinement.

2. Materials and methods

2.1. Enzyme purification

A plasmid containing the rmCK gene was transformed into *Escherichia coli* BL21(DE3)pLysS cells and creatine kinase was purified by affinity chromatography using a Cibracron Blue 3GA agarose column as described previously (Chen *et al.*, 1996). The purified enzyme was concentrated by ultrafiltration and exchanged into 20 m*M* Tris pH 8.1 with 0.1 m*M* EDTA. The CK mutants were each found to be >99% pure by SDS–PAGE (BioRad). Enzyme concentrations were measured by absorbance at 280 nm (ε = 75 600 cm^{-1} M^{-1}; Kuby *et al.*, 1954).

2.2. Crystallization, data collection and processing

The enzyme form examined in this study is a highly soluble rmCK mutant (R134K) that is active and quite stable. The creatine kinase mutants were cloned, expressed and purified as described previously (Chen *et al.*, 1996) and stored at 277 K as a 130 mg ml^{-1} stock solution during complex formation and prior to crystallization trials. Assays on the native, R134K, Δ1–15 and P20G mutants were conducted as described previously (Chen *et al.*, 1996). The enzyme samples were diluted to a final concentration of 24 mg ml^{-1} in a buffer consisting of 12.5 m*M* sodium nitrate, 6.25 m*M* magnesium

acetate, 6.25 m*M* ADP, 1.5 m*M* creatine and 25 m*M* HEPES buffer pH 7.5 and incubated on ice for 1 h prior to crystallization. The enzyme was pre-incubated with the transition-state analog (TSA) components creatine, nitrate and MgADP and then screened for crystallization conditions. Crystals were grown at room temperature using the hanging-drop vapor-diffusion method from a solution consisting of 20% PEG 8K, 25 m*M* ammonium acetate, 25 m*M* sodium nitrate and 0.1 *M* sodium cacodylate pH 6.5 in 1 + 1 µl drops suspended over an 800 µl well. Synchrotron X-ray diffraction data were collected at a wavelength of 1.00 Å at 100 K on the Industrial Macromolecular Crystallography Association (IMCA) beamline 17-ID at the Advanced Photon Source, Argonne National Laboratory. Diffraction data were processed using *DENZO* and *SCALEPACK* from the *HKL*-2000 program suite (Otwinowski & Minor, 1997). The space group was determined to be primitive orthorhombic $P2_12_12_1$ with two molecules per asymmetric unit, corresponding to a solvent content of 42.7% (Matthews, 1974).

2.3. Structure determination and refinement

The structure was solved by the molecular-replacement method with the native rabbit muscle structure (PDB code 2crk) as a search model using the program *MOLREP* from the *CCP*4 suite (Collaborative Computational Project, Number 4, 1994; Rao *et al.*, 1998; Rossmann & Blow, 1962; Vagin & Teplyakov, 1997). Structural refinement and calculation of electron-density maps took place using the program *REFMAC*5 from the *CCP*4 suite, using the complete data with no resolution or σ-cutoff (Collaborative Computational Project, Number 4, 1994; Murshudov *et al.*, 1997; Rao *et al.*, 1998). Manual fitting and real-space refinement of the protein model was performed using the program *QUANTA*-2000 (Accelrys Inc., San Diego, CA, USA). The asymmetric unit of the rmCK structure contains two monomers that can be superimposed by a 92° rotation around a pseudo-symmetry axis. Cytosolic CKs are functional homodimers; therefore, this crystal structure is likely to represent the functional biological unit. The final crystallographic model contains two complete polypeptide chains from residues 1–380, as well as two MgADP molecules, one creatine and one nitrate. The model fits the 1.65 Å resolution data quite well, with an R_{work} of 16.7% and an R_{free} of 20.0% after refinement. Data-collection and crystallographic refinement statistics are summarized in Table 1. Analysis of the Ramachandran plot showed that 91.3% of the residues fall in the most favored regions, with 8.1% in additionally allowed regions, 0.6% in generously allowed region (two Glu231 residues in the active sites) and no residues in the disallowed regions, as defined by *PROCHECK* (Laskowski *et al.*, 1993).

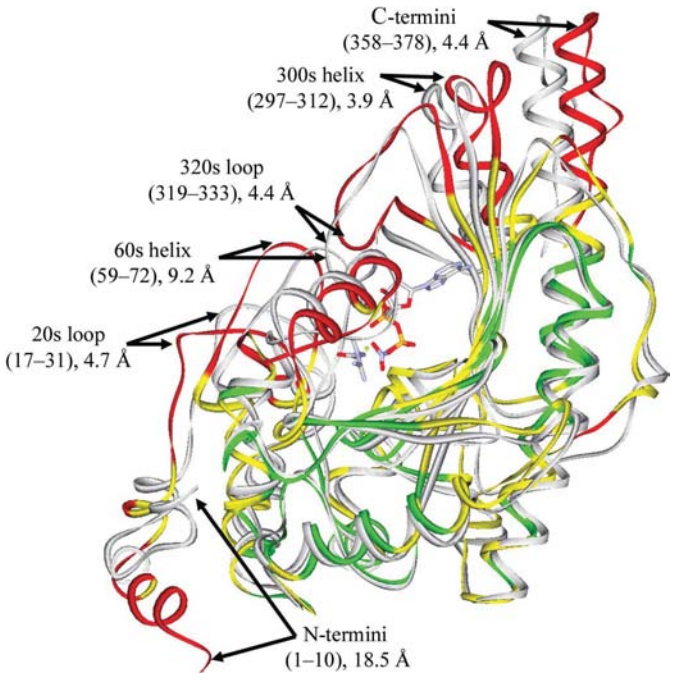

Figure 1
Superposition of the two monomers illustrates the structural asymmetry. A ribbon diagram of the ADP-bound monomer is shown rotated 92° around the pseudo-symmetry axis and superimposed on the TSA-bound monomer colored gray. The ADP-bound monomer is colored according to the r.m.s. differences between the main-chain atoms: differences greater than 2.5 Å are shaded red, differences between 1.3 and 2.4 Å are shaded yellow and differences less than 1.3 Å are shaded green. The structural elements that have the maximum positional differences between the two conformations are annotated.

2.4. Structure analysis

Structural analysis and preparation of figures was performed using *Discovery Studios Modeling* (Accelrys Inc., San Diego, CA, USA). Additional structural analysis was performed using the web-based interface for *DynDom* located at http://www.sys.uea.ac.uk/dyndom (Hayward & Berendsen, 1998). Sequence and structural-based alignments were performed using the web-based interface to *ESPript* 2.2 located at http://espript.ibcp.fr/ESPript/ESPript (Gouet *et al.*, 1999).

3. Results and discussion

3.1. Overall structure

We have examined the high-resolution structure of a transition-state analog complex of a creatine kinase mutant (R134K) in order to assess the role of key structural elements in active-site communication and catalytic regulation. While there are a cluster of conserved arginines involved in nucleotide binding (Jourden *et al.*, 2005), Arg134 in the native enzyme is fully buried within the mantle of CK and fulfills an important structural role (Cox *et al.*, 2003). This mutant has a similar CD spectrum as the native enzyme and a slightly lower thermal stability, while possessing high catalytic efficiency (about one-third of the native k_{cat}/K_m; Table 2). The R134K mutant is extremely soluble, with stock protein concentrations of >100 mg ml^{-1} easily being achieved. This high solubility has allowed us to examine a greater range of crystallization conditions and led to the production of highly ordered single crystals of this enzyme form.

Table 2
Kinetics of creatine kinases.

Data were fitted to a rapid-equilibrium random-order mechanism (Borders *et al.*, 2002).

Enzyme form	k_{cat} (s^{-1})	MgATP K_d (m*M*)	MgATP K_m (m*M*)	Creatine K_d (m*M*)	Creatine K_m (m*M*)	Relative $k_{cat}/(K_{dA}K_{mC})$
Native	147.7 ± 4.8	1.0 ± 0.25	0.73 ± 0.09	12.4 ± 3.4	9.0 ± 0.9	1.00
R134K	73.5 ± 2.7	0.78 ± 0.09	0.93 ± 0.07	15.5 ± 2.0	18.5 ± 1.3	0.31
P20G	3.2 ± 0.3	7.7 ± 2.9	0.94 ± 0.69	260 ± 230	33 ± 9	9.7×10^{-5}

The structure of rabbit muscle-type creatine kinase determined in this study shares a similar overall structural topology to other guanidino kinases. There is a smaller primarily α-helical amino-terminal domain and a larger α/β saddle carboxyl-terminal domain containing the active-site cleft. In contrast to the crystal structure of the apo form of the homodimer of rmCK, which consists of two identical monomers related by crystallographic symmetry (Rao *et al.*, 1998), there is significant asymmetry observed between the two subunits. In this new rmCK structure, one monomer exists in the closed conformation with the active site occupied by the fully formed TSA complex (rmCK–TSA). The other monomer is in a more open conformation with only MgADP in the active site (rmCK–ADP) and no evidence of either bound creatine or nitrate. The structure of the rmCK–TSA subunit is well ordered, with unambiguous density from the first residue (Pro1) to the last (Lys380). The rmCK–ADP subunit is somewhat more flexible but still complete, with isotropic displacements (*B* factors) for the main-chain atoms averaging around 22 Å^3 compared with 14 Å^3 for the rmCK–TSA monomer. Superimposition of the two subunits reveals significant structural differences between these two monomers (Fig. 1). These differences provide some important and unexpected insights into the catalytic and regulatory mechanisms of CK.

3.2. Structural differences exist between the monomers

Although rmCK was cocrystallized in the presence of saturating levels (greater than ten times the K_m or K_i) of each of the TSA components (Borders *et al.*, 2002), only one subunit is found to be occupied by the completely formed TSA complex. This subunit asymmetry in the functional homodimer has previously been reported for the unliganded chicken brain CK (cbCK) structure and the *T. californica* creatine kinase (*tc*CK) TSA-complex structure, but has not been observed in apo muscle-type CK structures (Eder *et al.*, 1999; Lahiri *et al.*, 2002; Rao *et al.*, 1998; Shen *et al.*, 2001).

Subunit asymmetry has also been observed in solution for muscle CK. Treatment of rabbit muscle CK with thiol-specific reagents led to differential modification of the monomers, with one of the active-site cysteines being significantly more reactive than the other (Degani & Degani, 1979, 1980). Derivatization of a single active-site cysteine also resulted in a loss of more than half of the catalytic activity, indicating that subunit interactions modulate the activity of CK (Grossman & Sellers, 1998). Similar cooperative activity losses were seen in the ATP-synthetic reaction of CK for heterodimers containing a single mutated subunit (Hornemann *et al.*, 2000).

Dynamic domain analysis was conducted in order to better understand the structural and functional differences between the two subunits, using the web-based interface of the program *DynDom* (Hayward & Berendsen, 1998). This analysis shows that when the two monomers are superimposed, the open conformation can be converted to the closed form by a 13° rotation of a single subdomain composed of five substructural elements around nine two-residue hinge points. These structural elements are interspersed between the N-terminal and C-terminal domains and are consistent with those present in the other phosphagen kinase structures. Two key structural differences that may potentially affect catalytic function become apparent when the two monomers are compared: changes in the position of two loop segments that function to control access to the active-site cleft and a dramatic difference in the conformation and position of the N-termini (Fig. 1).

3.3. Role of loop conformations in controlling active-site access

The two loop segments involved in 'closing' the CK active site upon substrate binding are composed of residues 59–72 (the 60s loop) and residues 319–333 (the 320s loop). The existence of a 'latch' between the 60s and 320s loop segments has been proposed based on the *tc*CK–TSA structure (Lahiri *et al.*, 2002; McLeish & Kenyon, 2005; Wang *et al.*, 2005). Because of the higher resolution of our rmCK structure, we can now examine the interactions involved in these conformational changes in greater detail. The 60s-loop region forms a major portion of the creatine pocket and undergoes a large change in conformational upon creatine binding in the TSA complex. Ile68, Thr70 and Val71, along with the other residues in this region, create a specificity pocket for creatine (Fig. 2; Novak *et al.*, 2004). These residues are highly conserved and differentiate CK from related guanidino kinase family members such as AK that are missing several residues in this region (Azzi *et al.*, 2004). The 60s loop locks the creatine substrate into position as a result of a 44° rotation around the hinge residues Gly64 on the N-terminal side of the loop and Gly72 on the C-terminal side. This rotation results in a maximum displacement of over 9 Å when comparing the position of C^α of Pro66, which lies at the apex of the loop (Fig. 1). Part of the driving force for this conformational change is the formation of additional internal hydrogen bonds within the loop that are not present in the rmCK–ADP 60s loop. A new electrostatic interaction is also formed between the side chain of His65 and the side-chain carboxylic acid of Asp325 within the 320s loop that further stabilizes the 'closed' form of the CK active site, thus linking the creatine-binding

pocket in the 60s-loop region to the 320s loop containing the nucleotide-binding pocket. In the rmCK-ADP subunit the 'open' conformation moves His65 out of position, allowing the side chain of His65 to form a hydrogen bond to the carbonyl of the adjacent residue Gly64. This leaves the carboxylate group of Asp325 in an open position exposed to solvent.

3.4. Transition-state stabilization and catalysis

The high-resolution and clear electron density for the well ordered TSA components allow a detailed examination of the active site of the rmCK structure (Fig. 3). The TSA components are precisely oriented in the CK active site through several key interactions, resulting in thermal factors for the substrate analogs that are comparable to those of the main-chain atoms in the active-site region. The distance between the β-phosphoryl O atom of ADP and the guanidino N atom *cis* to the creatine methyl group, measured through the center of mass of the bound nitrate, is 6.1 Å (Fig. 3*b*). The position of the planar nitrate, stabilized by the ADP-bound magnesium ion, is nearly equidistant between the phosphoryl donor and acceptor atoms.

Glu231 has been proposed to act as the catalytic base that abstracts a proton from the nucleophilic N atom of the creatine guanidino group (Cantwell *et al.*, 2001; Eder *et al.*, 2000). However, mutational studies at this position conducted on both CK and AK suggest that an acid/base catalytic role for Glu231 in guanidino kinases may not be as important as its role in the precise alignment of the substrates (Pruett *et al.*, 2003). The side-chain carboxyl group of Glu231 forms a strong bidentate electrostatic interaction with the guanidino group of creatine that serves to orient the substrate in the correct location for catalysis (Fig. 2). In fact, the peptide plane of Glu231 in both the rmCK–ADP and rmCK–TSA active sites is found in a strained conformation that is required to correctly position the side-chain carboxylate in the active site. Interestingly, this strained geometry is also observed in the absence of creatine both in this structure and in the high-resolution structure of the brain isoform of CK (Eder *et al.*, 1999), supporting the argument for a pre-formed active site to facilitate substrate binding.

Our structural studies of the TSA complexes show that only one monomer in the CK homodimer can be occupied by creatine at any given time. Because of this asymmetry in substrate binding, structural differences are to be expected in the area around the creatine-binding pocket. However, large differences between the subunits are also observed in the nucleotide-binding site despite the presence of MgADP in both monomers. MgADP in the rmCK–TSA complex is very tightly bound in a 'closed' ATP pocket with *B* factors that are equivalent to the protein main-chain atoms. However, the *B* factors for the MgADP molecule in the other subunit are three times larger. The large decrease in entropy required for the binding of MgADP is offset by the dramatic increase in the enthalpy of binding that arises from the additional hydrogen-bonding and hydrophobic interactions that are formed by the collapse of the creatine kinase active site around the active-site components in the rmCK–TSA subunit. A base-stacking interaction is formed between the side chain of His295, which has previously been identified as playing a critical role in catalysis (Chen *et al.*, 1996), and the adenosine ring of ADP in the active site of both subunits (Fig. 2). The exocyclic amine on C6 forms a hydrogen bond to the backbone carbonyl O atom of Gly293, both the side chain of His190 and the main-chain carbonyl O atom of Thr321 form hydrogen bonds to the 3′-hydroxyl group of the ribose ring and the 2′-hydroxyl interacts with the backbone carbonyl of Ile187 through an intervening water molecule (Fig. 2). These numerous electrostatic interactions, combined with the increased van der Waals contacts resulting from the exclusion of water from the active site, explains the lower thermal factors observed for ADP in the TSA complex and provide structural support for the synergistic binding that is observed with the substrates of CK (Borders *et al.*, 2002).

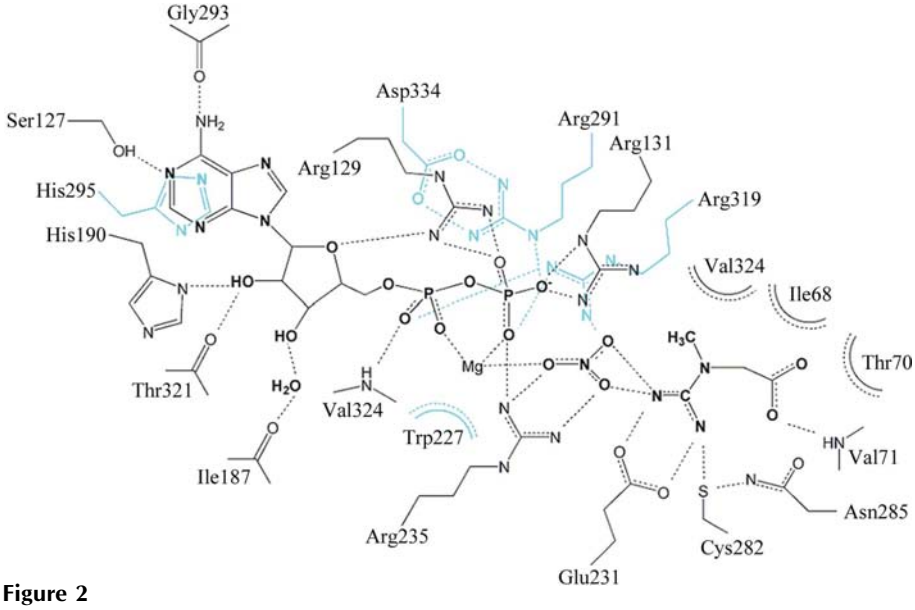

Figure 2
Annotated active-site diagram of the transition-state analog complex of muscle creatine kinase. Hydrogen bonds with distances ranging from 2.7 to 3.0 Å are indicated by dotted lines, while van der Waals interactions are indicated by curved dashed lines. The magnesium–oxygen coordination distances are 2.1–2.3 Å. Residues colored cyan are located at the back of the pocket with respect to the TSA components.

In response to this tight fit within the active site, the β-phosphate group of MgADP adopts a different conformation in each of the subunits. In the rmCK–ADP site the β-phosphate O atoms are in a lower energy staggered conformation relative to the position of the α-phosphate O atoms. However, in the rmCK–TSA site the β-phosphate O

atoms of MgADP are in a higher energy eclipsed conformation (Fig. 3). This eclipsed conformation was also observed in the TSA complexes of *tc*CK and AK (Lahiri *et al.*, 2002; Yousef *et al.*, 2002) and is likely to serve to accelerate the departure of the phosphoryl group that is transferred during the catalytic cycle.

3.5. Dimerization and the role of the amino-terminus in subunit association

All cytosolic creatine kinases examined to date are found as functional dimers, while the closely related arginine kinases are active as monomers. The biochemical basis for the higher level of organization for CK has not been fully explained. However, the importance of dimerization in CK activity is highlighted by the report of a lethal D54G mutation in CK (Yamamichi *et al.*, 2001). Removal of the carboxylate group in the D54G mutant results in a destabilization of the dimer interface. Monomeric rmCK has been shown to retain a small amount of basal activity (Cox *et al.*, 2003), indicating that dimerization of CK is not absolutely required for its *in vitro* activity; however, disruption of dimer formation leads to dramatically reduced catalytic efficiency. Several gene-truncation studies have examined the potential role of the N-terminal region of CK in subunit association and catalytic activity, with mixed results having been reported. Removal of the first five residues of MiCK (MiCK Δ1–5) was shown to produce an active form of the mitochondrial enzyme, but with a 30-fold reduced association constant for the octameric form over the dimeric form (Kaldis *et al.*, 1994). In contrast, removal of the first six residues of the muscle enzyme (rmCK Δ1–6) resulted in retention of the homodimer. This truncated enzyme form has ∼70% of the native activity and increased thermal stability (Guo *et al.*, 2003).

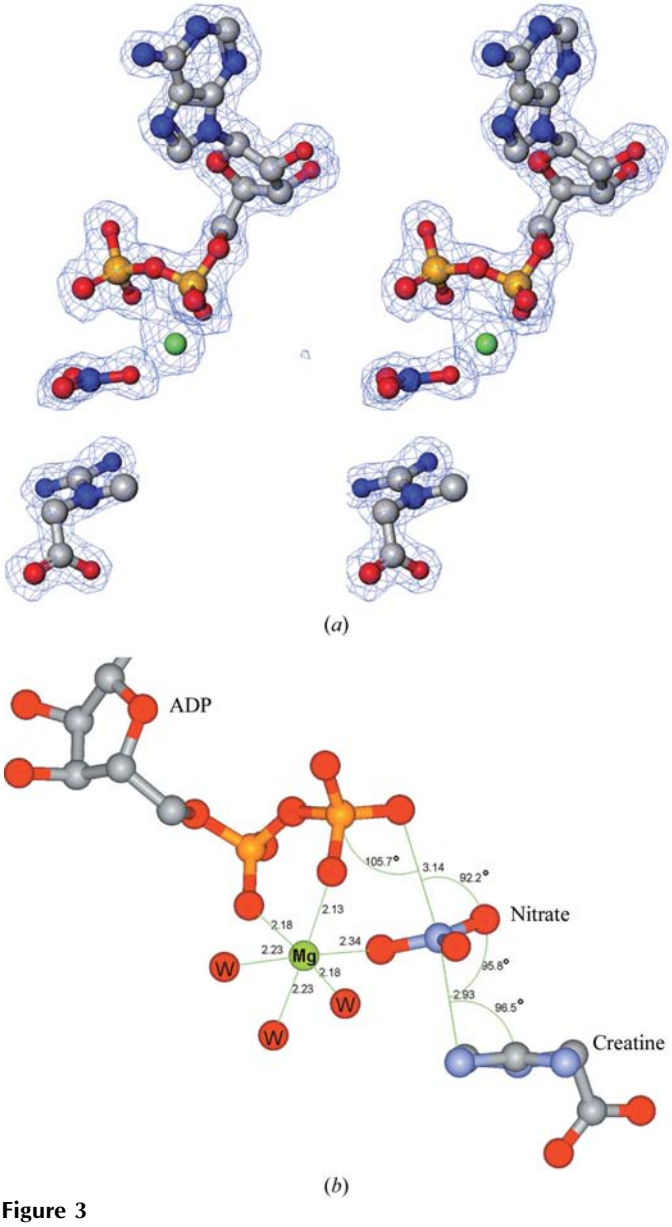

Figure 3
Detailed view of the enzyme-bound TSA components. (*a*) Refined positions of the TSA components surrounded by an unbiased $F_o - F_c$ OMIT map contoured at 3σ. (*b*) The TSA components are shown with bond lengths and bond angles between the β-phosphoryl group of ADP, the planar nitrate group and the guanidino N atom of creatine that accepts the transferred phosphoryl group.

An examination of our high-resolution structure shows that Asp54 in the rmCK–ADP subunit forms a hydrogen bond to the side chain of His6 in the adjacent rmCK–TSA subunit, while Asp54 from the rmCK–TSA subunit forms a hydrogen bond to the backbone N atom of Pro1 within the same chain. The loss of this critical hydrogen bond must be sufficient to cause dissociation of the dimer. Our structural data also provide additional details on the participation of the amino-terminal region of CK in homodimer formation. A *PDBsum* analysis (Laskowski *et al.*, 1993) of the protein–protein contacts in the rmCK dimeric structure indicate that 40 residues from each monomer contribute to a solvent-excluded area of ∼1900 Å^2. There are a total of 32 hydrogen bonds and over 250 van der Waals contacts that make up the dimer interface, with 30% of the interactions provided by the first 20 residues of the rmCK–ADP monomer and 50% of the interactions provided by the first 20 residues of the rmCK–TSA monomer.

When the two subunits are superimposed, the positions of the respective N-terminal amino acids are separated by nearly 19 Å owing to a rotation of ∼72° measured from the backbone carbonyl of Tyr9 to the backbone carbonyl of Pro1 (Fig. 1). The positional differences between the first ten residues of the N-terminal region of CK in the open and closed forms are dramatic and were not observed in the previous *tc*CK structure owing to the lack of interpretable electron density in this region (Lahiri *et al.*, 2002). The N-terminus of the rmCK–ADP monomer lies along a hydrophobic groove of the adjacent rmCK–TSA monomer, while the first six residues of the rmCK–TSA N-terminus are wedged into the homodimer interface and shielded from solvent. To accommodate the first six residues of the N-terminus of the rmCK–TSA monomer, the termini of the adjacent rmCK–ADP must move away from the active site. The 'tucked-in' position of the N-terminal residues found in this structure is likely to be an accurate reflection of the solvent structure since *in vitro* experiments

found that both of the N-termini of CK are protected from chemical denaturation (Guo *et al.*, 2002; Pineda & Ellington, 1999). The change in the position of the N-terminus of rmCK–TSA is accompanied by a partial unwinding of the helix, creating additional space that may allow the movement of the 20s loop and in particular allow residues His25, Asn26, Asn27 and His28 to move in response to substrate binding. These residues are fully conserved in all CKs (Edmiston *et al.*, 2001), but the corresponding residues are not conserved in the AK family, consistent with the essential role of this region in CK subunit association.

3.6. Functional examination of the amino-terminus

Our high-resolution structure of rmCK shows that the amino-terminus (in particular residues 1–22) forms extensive contacts within the dimer interface, suggesting that the removal of these residues should result in a decrease in dimer stability. To shed additional light on the role of the amino-terminus in subunit association, a truncated form of rmCK with the first 15 amino-terminal residues removed (rmCK Δ1–15) was cloned, expressed in *E. coli*, purified and kinetically characterized. Consistent with this hypothesis, the rmCK Δ1–15 enzyme form causes a disruption in subunit association, leading to an enzyme that purifies as a monomer with significantly reduced enzymatic efficiency. Size-exclusion chromatography studies show that this truncated enzyme exists in a concentration-dependent equilibrium between the monomeric and dimeric forms. The resulting kinetic time course is nonlinear as a consequence of the dissociation of the dimer upon dilution into the assay reaction mixture. The specific activity of the dimeric form is estimated to be about 29 U mg^{-1} from the initial velocities, while the specific activity of the dissociated monomer is only 2.6 U mg^{-1}, compared with >100 U mg^{-1} for the native enzyme.

Sequence alignment and structural data suggest that this dissociation into monomers may partly be a consequence of a destabilization of the conserved α-helix 1 in CK which begins at residue His6 (Fig. 4). Analysis of the superimposed monomers in the rmCK structure suggests that Pro20 may function as a hinge point to accommodate the large conformational changes seen in the N-terminal region (Fig. 1). Pro20 is highly conserved in oligomeric CKs, but is not conserved in the related arginine kinases, which function almost exclusively as monomers. In order to assess the importance of this residue and its role in CK function, a P20G mutant was cloned, expressed in *E. coli*, purified and tested for activity. Surprisingly, the increased flexibility present in the P20G mutant completely disrupts subunit association, leading to a monomer with a specific activity of only ∼0.6 U mg^{-1}.

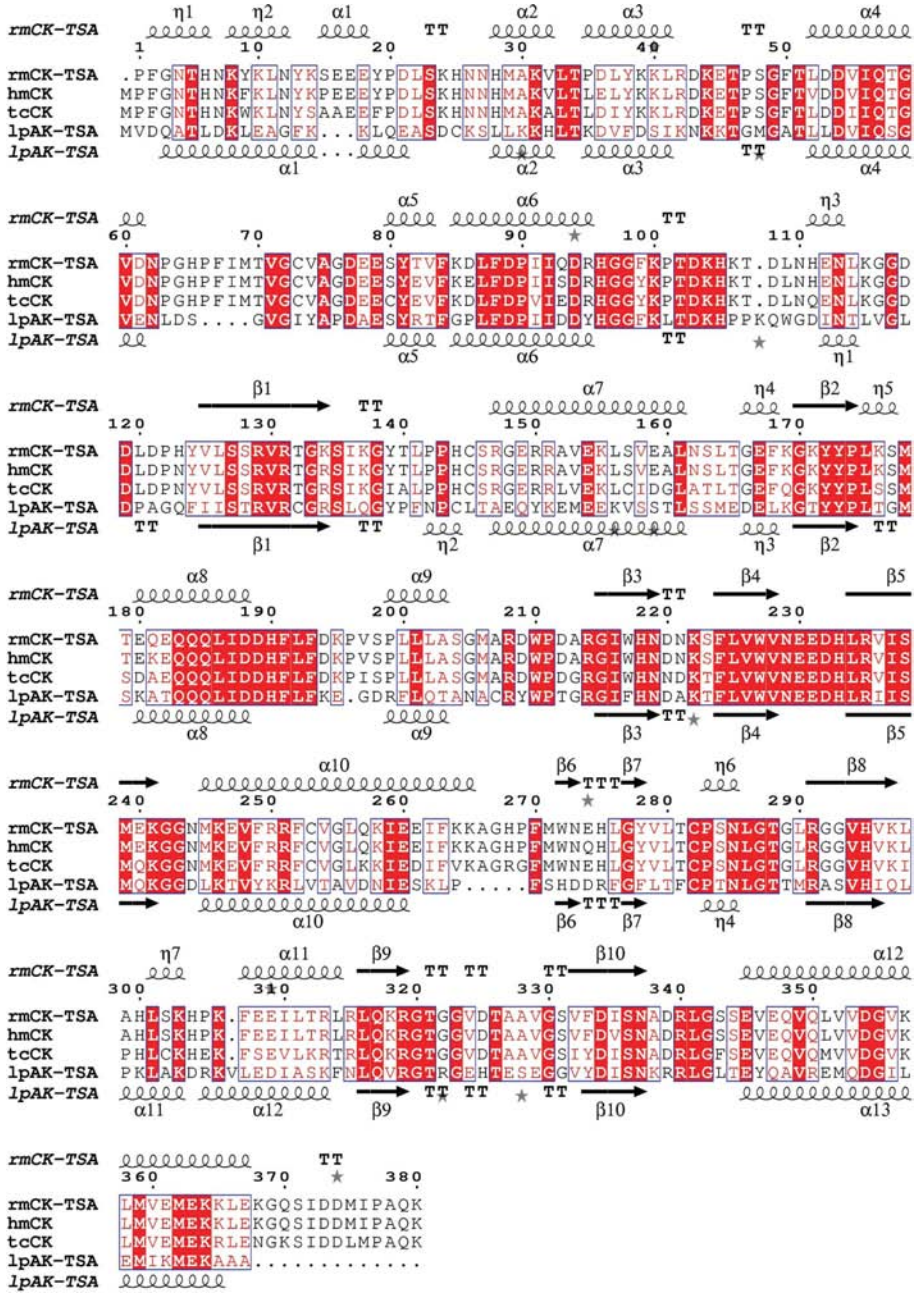

Figure 4
Sequence and structural alignment of muscle-type creatine kinase with arginine kinase. The sequence and secondary-structural alignment shows the rmCK (R134K) mutant determined in this report (PDB code 1u6r) compared with human muscle-type CK (PDB code 1ioe; Shen *et al.*, 2001), California electric ray CK (PDB code 1vrp; Lahiri *et al.*, 2002) and horseshoe crab AK (PDB code 1m15; Yousef *et al.*, 2002). The secondary-structural elements for the rmCK–TSA monomer and the AK–TSA complex are compared at the top and bottom of the sequences, respectively.

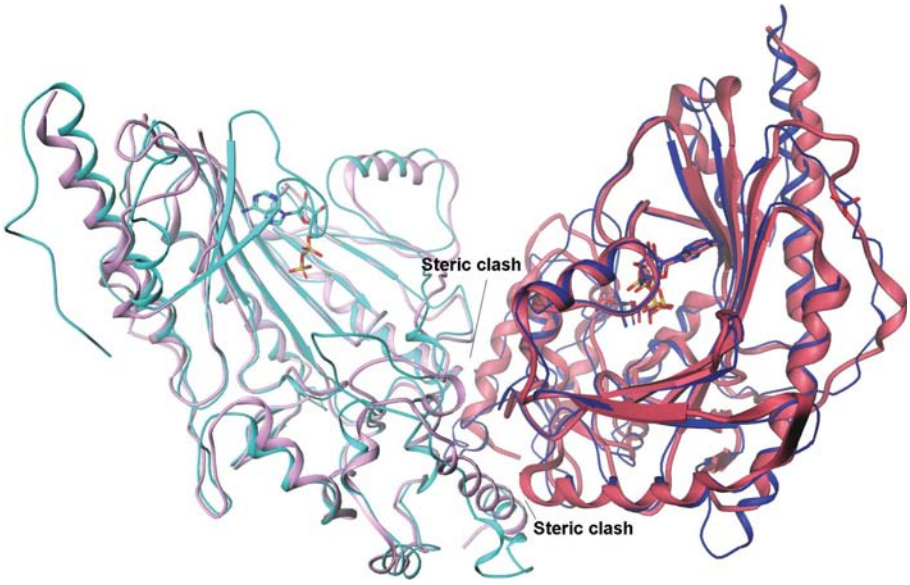

Figure 5
Overlay of a model of an AK dimer superimposed onto the rmCK dimer. In order to create the AK dimer, the AK–TSA complex (PDB code 1m15, red ribbon; Yousef *et al.*, 2002) was superimposed onto the rmCK–TSA monomer (dark blue ribbon) and the apo AK monomer (PDB code 1m80, pink ribbon; Yousef *et al.*, 2003) was superimposed onto the rmCK–ADP monomer (light blue ribbon).

The results of these combined studies support the importance of the N-terminal domain of CK in subunit association and in enzymatic activity.

3.7. Comparison between the CK dimer and the AK monomer

A comparison of the open and closed forms of rmCK observed in this study with the apo (open) and TSA-bound (closed) structures of arginine kinase reveals that AK has a 20-residue α-helical segment in the N-terminus instead of the conformationally flexible N-terminal region of CK (Yousef *et al.*, 2003). In contrast to the large conformational changes that occur in CK upon binding of the TSA components, the N-terminal region of AK remains essentially unchanged between the open and closed conformations. This extended N-terminal helix found in AK is likely to interfere with the subunit interactions required to stabilize dimer formation. A putative AK dimer model was constructed by superimposing the AK–TSA complex (Yousef *et al.*, 2002) onto the rmCK–TSA monomer and the apo AK monomer onto the rmCK–ADP monomer. The resulting AK dimer model has two significant steric clashes that are likely to prevent homodimer formation, with the C^{α}-backbone trace of N-terminal helix 1 of AK approaching within $\sim$2 Å of the C^{α} trace of helix 7 (Fig. 5). These steric clashes observed in the model of the putative AK dimer may be the reason why both AK and the rmCK P20G mutant, which can potentially form an extended N-terminal helix, cannot exist as stable homodimers.

3.8. Intersubunit communication in CK

This observation raises the question of how AK is able to function so efficiently as a monomer while the closely related CK monomers have significantly reduced catalytic activity. Based on the structural analysis of these two phosphagen kinase families, we propose that CK has evolved to function as a dimer by using its N-terminal domain to support communication between the subunits. Our new structure confirms the presence of a link between the active site of the two monomers of the functional CK homodimer. Asn27 in the rmCK–TSA complex forms hydrogen bonds with Gly59 and Asn62, two residues in the 60s loop that form the creatine-binding pocket (Novak *et al.*, 2004; Wang *et al.*, 2005). Asn26 in the rmCK–TSA monomer forms a water-mediated interaction with the side chain of Thr70, shifting this side chain out of the creatine pocket to allow the substrate to bind. In the rmCK–ADP monomer Asn27 no longer interacts with Asn62 while Asn26 is now found to form a hydrogen bond with the backbone carbonyl of His65 instead of with Thr70. In the absence of this interaction, the side chain of Thr70 rotates back into the empty creatine pocket of the rmCK–ADP active site, preventing the phosphagen substrate from productive binding. His65 is part of the highly conserved PGHP motif and has been proposed to perform a key role in phosphagen specificity and catalysis (Azzi *et al.*, 2004; Novak *et al.*, 2004; Wang *et al.*, 2005). Thus, both Asn26 and Asn27 seem to play key roles in signal transmission and these interactions link movements in the N-terminal domain to the loop that controls entry into the enzyme active site. Information regarding the occupancy of the active site can therefore be communicated from the 60s-loop region through Asn26 and Asn27 to the N-terminal domain of one CK monomer and then, through the interactions between adjacent N-termini described above, to the active site of the adjacent monomer.

4. Conclusions

Analysis of this high-resolution structure of the transition-state analog complex of a mammalian muscle form of creatine kinase and the subsequent kinetic studies of the rmCK Δ1–15 and P20G mutants provides detailed evidence that the amino-terminal region of CK is intimately involved in subunit association, subunit communication and enzymatic activity.

We thank Barry Finzel for his thoughtful review of the manuscript. Krystal Davis prepared the P20G mutant and Daniel Pipitone and Mark Snider (College of Wooster) carried out the kinetic analysis of these mutants. The work conducted at the College of Wooster was supported by an NSF grant (0344432). Use of the Advanced Photon Source was supported by the US Department of Energy, Basic Energy Sciences,

Office of Science under Contract No. W-31-109-Eng-38. Access to the IMCA-CAT facilities are supported by the companies of the Industrial Macromolecular Crystallography Association through a contract with Illinois Institute of Technology (IIT), executed through IIT's Center for Synchrotron Radiation Research and Instrumentation.

References

Azzi, A., Clark, S. A., Ellington, W. R. & Chapman, M. S. (2004). *Protein Sci.* **13**, 575–585.

Borders, C. L., Snider, M. J., Wolfenden, R. & Edmiston, P. L. (2002). *Biochemistry*, **41**, 6995–7000.

Cantwell, J. S., Novak, W. R., Wang, P. F., McLeish, M. J., Kenyon, G. L. & Babbitt, P. C. (2001). *Biochemistry*, **40**, 3056–3061.

Chen, L. H., Borders, C. L., Vásquez, J. R. & Kenyon, G. L. (1996). *Biochemistry*, **35**, 7895–7902.

Collaborative Computational Project, Number 4 (1994). *Acta Cryst.* D**50**, 760–763.

Cox, J. M., Davis, C. A., Chan, C., Jourden, M. J., Jorjorian, A. D., Brym, M. J., Snider, M. J., Borders, C. L. & Edmiston, P. L. (2003). *Biochemistry*, **42**, 1863–1871.

Degani, C. & Degani, Y. (1980). *J. Biol. Chem.* **255**, 8221–8228.

Degani, Y. & Degani, C. (1979). *Biochemistry*, **18**, 5917–5923.

Eder, M., Schlattner, U., Becker, A., Wallimann, T., Kabsch, W. & Fritz-Wolf, K. (1999). *Protein Sci.* **8**, 2258–2269.

Eder, M., Stolz, M., Wallimann, T. & Schlattner, U. (2000). *J. Biol. Chem.* **275**, 27094–27099.

Edmiston, P. L., Schavolt, K. L., Kersteen, E. A., Moore, N. R. & Borders, C. L. (2001). *Biochim. Biophys. Acta*, **1546**, 291–298.

Fritz-Wolf, K., Schnyder, T., Wallimann, T. & Kabsch, W. (1996). *Nature (London)*, **381**, 341–345.

Gouet, P., Courcelle, E., Stuart, D. I. & Metoz, F. (1999). *Bioinformatics*, **15**, 305–308.

Grossman, S. H. & Sellers, D. S. (1998). *Biochim. Biophys. Acta*, **1387**, 447–453.

Guo, S. Y., Wang, Z., Ni, S. W. & Wang, X. C. (2003). *Biochimie*, **85**, 999–1005.

Guo, Z., Wang, Z. & Wang, X. C. (2002). *Biochemistry (Mosc.)*, **67**, 1388–1394.

Hayward, S. & Berendsen, H. J. C. (1998). *Proteins*, **30**, 144–154.

Hornemann, T., Rutishauser, D. & Wallimann, T. (2000). *Biochim. Biophys. Acta*, **1480**, 365–373.

Jourden, M. J., Geiss, P. R., Thomenius, M. J., Horst, L. A., Barty, M. M., Brym, M. J., Mulligan, G. B., Almeida, R. M., Kersteen, B. A., Myers, N. R., Snider, M. J., Borders, C. L. & Edmiston, P. L. (2005). *Biochim. Biophys. Acta*, **1751**, 178–183.

Kaldis, P., Furter, R. & Wallimann, T. (1994). *Biochemistry*, **33**, 952–959.

Kuby, S. A., Noda, L. & Lardy, H. (1954). *J. Biol. Chem.* **209**, 191–201.

Lahiri, S. D., Wang, P. F., Babbitt, P. C., McLeish, M. J., Kenyon, G. L. & Allen, K. N. (2002). *Biochemistry*, **41**, 13861–13867.

Laskowski, R. A., MacArthur, M. W., Moss, D. S. & Thornton, J. M. (1993). *J. Appl. Cryst.* **26**, 283–291.

McLeish, M. J. & Kenyon, G. L. (2005). *Crit. Rev. Biochem. Mol. Biol.* **40**, 1–20.

Matthews, B. W. (1974). *J. Mol. Biol.* **82**, 513–526.

Morrison, J. F. & James, E. (1965). *Biochem. J.* **97**, 37–52.

Murshudov, G. N., Vagin, A. A. & Dodson, E. J. (1997). *Acta Cryst.* D**53**, 240–255.

Novak, W. R. P., Wang, P. F., McLeish, M. J., Kenyon, G. L. & Babbitt, P. C. (2004). *Biochemistry*, **43**, 13766–13774.

Otwinowski, Z. & Minor, W. (1997). *Methods Enzymol.* **276**, 307–326.

Pineda, A. O. & Ellington, W. R. (1999). *Eur. J. Biochem.* **264**, 67–73.

Ponticos, M., Lu, Q. L., Morgan, J. E., Hardie, D. G., Partridge, T. A. & Carling, D. (2004). *EMBO J.* **17**, 1688–1699.

Price, N. C. & Hunter, M. G. (1976). *Biochim. Biophys. Acta*, **445**, 364–376.

Pruett, P. S., Azzi, A., Clark, S. A., Yousef, M. S., Gattis, J. L., Somasundaram, T., Ellington, W. R. & Chapman, M. S. (2003). *J. Biol. Chem.* **278**, 26952–26957.

Rao, J. K., Bujacz, G. & Wlodawer, A. (1998). *FEBS Lett.* **439**, 133–137.

Rossmann, M. G. & Blow, D. M. (1962). *Acta Cryst.* **15**, 24–31.

Schlattner, U., Tokarska-Schlattner, M. & Wallimann, T. (2006). *Biochim. Biophys. Acta*, **1762**, 164–180.

Shen, Y., Tang, H., Zhou, H. & Lin, Z. (2001). *Acta Cryst.* D**57**, 1196–2000.

Suzuki, T. & Furukohri, T. (1994). *J. Mol. Biol.* **237**, 353–357.

Vagin, A. A. & Teplyakov, A. (1997). *J. Appl. Cryst.* **30**, 1022–1025.

Wallimann, T., Wyss, M., Brdiczka, D., Nicolay, K. & Eppenberger, H. M. (1992). *Biochem. J.* **281**, 21–40.

Wang, P. F., Flynn, A. J., McLeish, M. J. & Kenyon, G. L. (2005). *IUBMB Life*, **57**, 355–362.

Wyss, M. & Kaddurah-Daouk, R. (2000). *Physiol. Rev.* **80**, 1107–1213.

Yamamichi, H., Kasakura, S., Yamamori, S., Iwasaki, R., Jikimoto, T., Kanagawa, S., Ohkawa, J., Kumagai, S. & Koshiba, M. (2001). *Clin. Chem.* **47**, 1967–1973.

Yousef, M. S., Clark, S. A., Pruett, P. K., Somasundaram, T., Ellington, W. R. & Chapman, M. S. (2003). *Protein Sci.* **12**, 103–111.

Yousef, M. S., Fabiola, F., Gattis, J. L., Somasundaram, T. & Chapman, M. S. (2002). *Acta Cryst.* D**58**, 2009–2017.

Zhou, G., Somasundaram, T., Blanc, E., Parthasarathy, G., Ellington, W. R. & Chapman, M. S. (1998). *Proc. Natl Acad. Sci. USA*, **95**, 8449–8454.